Fabrication and characterization of Co, Al:ZnO thin films by a sol-gel spin coating technique for ferromagnetic applications

R. Siddheswaran[a,*], **R.V. Mangalaraja**[a,*], **Ricardo E. Avila**[b], **Maria Elena Gómez**[c], **D.Manikandan**[a], **Marta Lopez**[a], **C. Esther Jeyanthi**[d] **and S. Ananthakumar**[e]

[a]*Advanced Ceramics and Nanotechnology Laboratory, Department of Materials Engineering, University of Concepcion, Concepcion, Chile*
[b]*Personal Dosimetry Section, Chilean Commission of Nuclear Energy, Santiago, Chile*
[c]*Department of Physics, University of Valle, Cali, Colombia*
[d]*Research and Development Centre, Bharathiar University, Coimbatore - 641 046, India*
[e]*Materials and Mineral Division, National Institute for Interdisciplinary Science and Technology, CSIR, Trivandrum-695019, Kerala, India*

Transparent polycrystalline ZnO and Co,Al co-doped ZnO [$Zn_{1-x-y}Co_xAl_yO$; x = 0.03; y = 0.02] thin films were fabricated using sol-gel spin coating on glass substrates and subsequently annealed at 500 °C for 2 h in an ambient atmosphere. The decomposition of the precursors and formation of the metal oxide during annealing was explained by thermal analysis. X-ray crystal diffraction analysis on the co-doped ZnO thin films confirmed the formation of the hexagonal wurtzite structure. Microstructural studies revealed that the films were filled with particulates of sizes ranging between 40-50 nm and with a uniform film thickness of about 700 nm after annealing at 500 °C. Atomic force microscopy (AFM) images demonstrated a fine and smooth surface of the thin films. The spin coated films have also been shown to possess polycrystalline grains with a compact and void-free morphology. The energy dispersive X-ray spectroscopic (EDS) analysis confirmed the presence of Co, Al, Zn and O. The room temperature (300 K) ferromagnetic behavior of Co, Al co-doped ZnO thin films is also discussed.

Key words: Co, Al: ZnO thin film, Spin coating, Morphology, Microstructure, Ferromagnetism.

Introduction

Transparent conducting oxides have been used extensively in transducers, solar cells, and semiconductor and optoelectronic devices. The efficiency of such devices is strongly linked to desirable key properties of materials such as high conductivity and transparency of the electrical contacts. Among the most promising materials, zinc oxide based materials standout as important materials in view of their high transmission over a wide spectral range and other interesting characteristics such as a relatively low cost and stability in reducing chemical environments. ZnO is of the hexagonal wurtzite structure with a direct wide band gap of 3.37 eV and an excitonic binding energy of ~ 60 meV, which permits the efficient excitonic stimulated UV emission even at room temperature (~ 25 meV) [1]. Extensive research has been made for wide band-gap semiconductors that have applications in photoconductors, fluorescence and optics. These are piezoelectric and transparent in the visible range and, can be made conducting with appropriate dopants like indium or aluminum to use in solar cells and flat panel displays [2, 3].

Zinc oxide based diluted magnetic semiconductors (DMS) have attracted much attention because of their theoretical predictions on room temperature ferromagnetism [4]. Doping selective elements in ZnO offers an effective way to adjust their optical, electrical and magnetic properties. Among these studies, Al doping in ZnO thin film can improve its conductivity without impairing the optical transmission, which is considered as the best candidate material for optoelectronics. ZnO films co-doped with Al and transition metals (TM) are important functional materials for optoelectronic and magneto-electronic applications [5, 6]. The transition metals generally used are Co and Mn [7, 8]. Al co-doped with transition metals in ZnO enhances its visible transparency, electrical conductivity and magnetic properties, which increases the interest for fabricating transparent electrodes [9-12].

Thin films of multi-component oxides with functional properties are very sensitive to the variations in the film morphological structure, such as porosity, grain boundaries, grain size and crystal structure (including the type and strength of the bonds). The preparation and doping conditions can control the structure, composition and hence the properties of the films. The sol-gel technique has advantages in fabricating DMS,

*Corresponding author:
 Tel : +56-41-2203664
 Fax: +56-41-2203391
 E-mail: rsiddhes@yahoo.com ; mangal@udec.cl

because the mole fractions can be controlled accurately with various compositions. The objective of the present study is to fabricate pure and Co, Al co-doped ZnO thin films on Corning glass substrates by a sol-gel spin coating process with a high pH. Also to study the structure, composition, morphology, thickness, thermal and magnetic properties of thin films in order to understand the physical grounds of their properties.

Experimental

Fabrication of Co, Al:ZnO thin films

The key to obtain a good quality thin films using the sol-gel spin coating method is the preparation of a clear, transparent and homogeneous solution. In this study, pure and Co,Al co-doped ZnO nanostructured thin films have been deposited on glass substrates. Fig. 1 shows a flow chart for the preparation of Co,Al : ZnO ($Zn_{1-x-y}Co_xAl_yO$; x = 0.03; y = 0.02) thin films. The precursor sols were made from zinc acetate dihydrate [$Zn(COOCH_3)_2.2H_2O$], isopropanol and monoethanolamine (MEA) as starting material, solvent and stabilizer, respectively. Cobalt nitrate hexahydrate ($Co(NO_3)_2.6H_2O$) and aluminum nitrate nonahydrate ($Al(NO_3)_3.9H_2O$) were introduced as dopants. The molar ratio of MEA to zinc acetate dihydrate was maintained at 1.0 and the concentration of zinc acetate was 0.95 M. The resultant mixed solution was allowed to stand at 60 °C for 2 h under stirring to yield a clear homogeneous solution. The as-prepared sol served as a coating solution after aging for 2 days at room temperature. The Corning glass substrates of dimensions 18 × 18 mm purchased from Sigma-Aldrich were sonicated and sequently rinsed with de-ionized water, ethanol and acetone. The coating solution was dropped on the glass substrates in a time interval of 5s using a Chemat KW-

4AD fluid dispenser. The precursor was deposited by spin coating for 30s (3000-4500 rpm) using a Chemat precision spin coater. For each coating, the film was dried at 120 °C for 10 minutes. The coating and drying process were repeated 8 times and then the thin films were annealed at 500 °C in a tubular furnace in an ambient condition at a heating rate of 5 K/minute for 2 h.

Characterization of Co, Al:ZnO thin films

The precursor solutions to be coated over the glass substrates were characterized by thermogravimetry and differential thermal analysis (TG/DTA) using a Netzsch -STA 409 PC/PG instrument to understand the effect of the thermal decomposition on the formation of ZnO thin films. The TG/DTA responses were recorded at a constant heating rate of 2 K/minute in a He atmosphere. The crystal structure of the thin films was confirmed by X-ray diffraction measurements carried out using a Siemens D5000 diffractometer, at a grazing incidence 2 ° off the sample plane with Cu-Kα radiation at 40 kV (20 mA). Data were collected at a scan step of 0.02 ° (2θ) with conditions of integration time of 4s per step over the 2θ scan range from 20 ° to 80 °. The crystallite sizes on the thin films were calculated for (101) peaks obtained from the diffraction patterns using full width at half maximum (FWHM) in the Debye-Scherrer formula [13]:

$$D = 0.9 \, \lambda \, / \, (\beta cos\theta) \tag{1}$$

where, D is the crystallite size in nanometer, λ is the wavelength of the incident X-ray (λ = 1.5406 Å), $\beta(\sqrt{\beta_s^2 - \beta_i^2})$ is the FWHM of the maximum intensive diffraction peak, and θ is the angle at which the maximum peak occurs. The surface microstructure and the thickness of the coated thin films were examined using scanning electron microscopy (SEM-JEOL 6460 LV) attached with an energy dispersive X-ray spectrometer and an atomic force microscope (AFM, model NT-MDT Solver Pro) operated in the semi-contact mode by a head scanner. Magnetic properties of the thin films were measured using a physical properties measurement system (PPMS, Quantum Design) in a vibrating sample magnetometer (VSM) mode.

Results and discussion

The thermal decomposition process of metal acetates and nitrates dissolved in isoproponal with monoethanolamine (MEA) shows the TGA (Fig. 2) and DTA (Fig. 3) traces towards the formation of pure ZnO and Co,Al:ZnO at 500 °C. It can be seen that the decomposition process consists of a few stages. From the TGA, it is found that both the materials show the same type of weigh losses and decomposition stages. In the DTA curve, only intense endothermic phenomena are observed until 300 °C where the weight loss ends and no other peaks are observed. The TGA shows three steps weight loss,
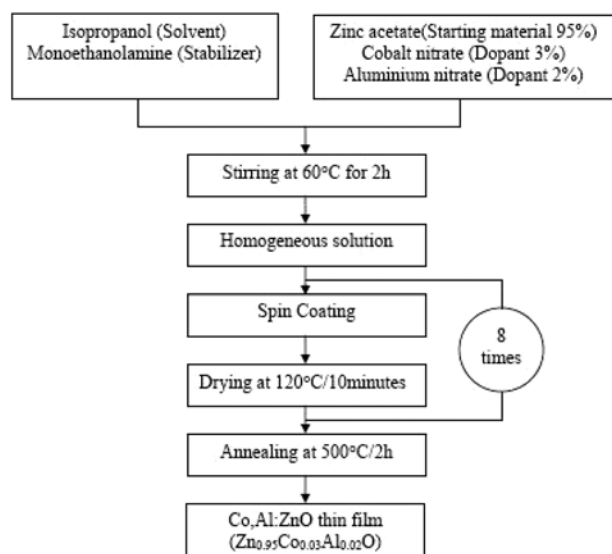

Fig. 1. Flow chart of the sol-gel method for preparation of Co, Al:ZnO thin films.
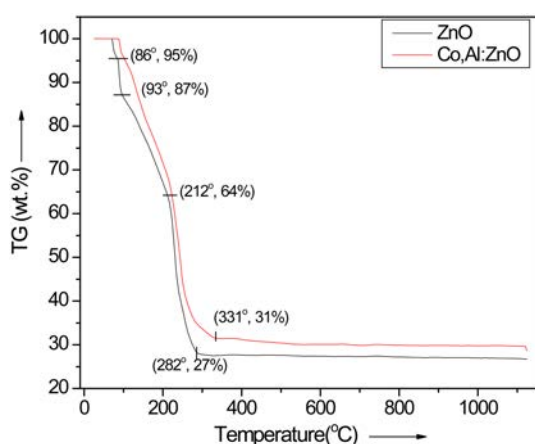
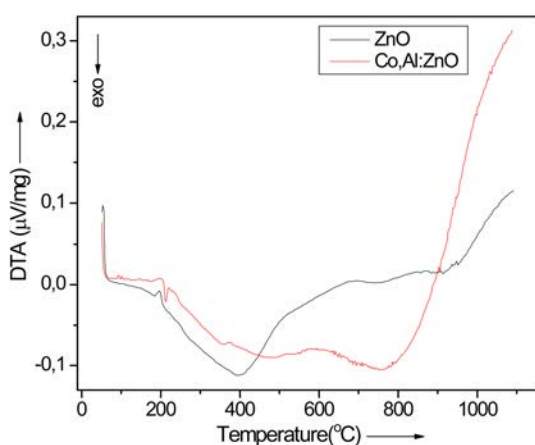**Fig. 2.** TGA traces of the pure ZnO and Co,Al:ZnO precursors.

Fig. 4. X-ray diffraction patterns of pure ZnO and Co,Al:ZnO thin films.

Fig. 3. DTA traces of pure ZnO and Co,Al:ZnO precursors.

Fig. 5. SEM micrographs of surfaces and cross-sectional areas of (a) ZnO and (b) Co,Al:ZnO thin films.

which begins at 86 $^{\circ}$C and is completed at 93 $^{\circ}$C leaving a residue of 87% of the initial weight, which is close to the decomposition of the weak bonded organic molecules in the solvents. This material goes through a further weight loss upto 300 $^{\circ}$C. From 93 $^{\circ}$C onwards water and other low molecular weight compounds are volatilized and, the organic material present in the acetate and nitrates are decomposed leaving a residue of 27% of the initial weight. The DTA shows two endothermic peaks form 90-200 $^{\circ}$C, due to the initiation of volatilization of water and low molecular weight organic compounds. Since the precursor of Co, Al:ZnO contains metal nitrates, the TGA trace (Fig. 2) exhibits an extended decomposition rather than the decomposition of precursor for the pure ZnO. Similar endothermic peaks are observed upto 200 $^{\circ}$C, simultaneously with a large weight loss upto 70% and the residue of 30% indicates the formation of metal oxide complexes. The huge exothermic hump at 400 $^{\circ}$C indicates the termination of volatilization and the formation of non-volatile metal oxides.

Fig. 4 shows the X-ray diffraction patterns of pure ZnO and Co, Al:ZnO thin films annealed at 500 $^{\circ}$C. It can be seen that both samples are polycrystalline and consist of single-phase ZnO (hexagonal wurtzite structure) with no in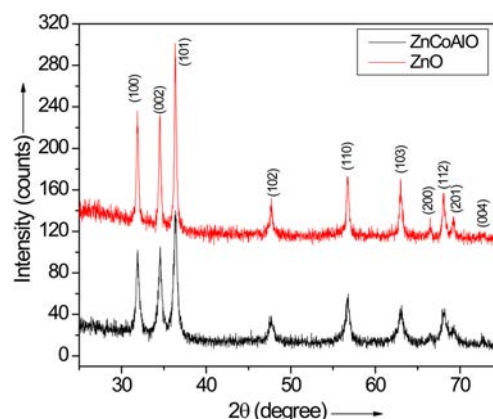dication of Co or Al oxides, or ternary (Co/ Al) ZnO phases. As seen in fig. 4, the narrow diffraction peaks in pure ZnO become broadened in Co, Al:ZnO due to the incorporation of the dopants. Also due to Co and Al doping, the concentration of the zinc interstitials are reduced for charge compensation which leads to a suppression of ZnO grain growth and deteriorates crystallinity [14].

It is observed that, the crystallite size in the Co, Al doped ZnO film is smaller than in the pure ZnO. This is attributed to the replacement of Zn^{2+} ions by Co^{2+} and Al^{3+} ions during formation of the Co and Al doped ZnO films. The radius of Al^{3+} ion is smaller than that of Zn^{2+} ion and radius of Co^{2+} is almost equal to Zn^{2+} ($rAl^{3+} = 0.054$ nm and $rZn^{2+} = 0.074$ nm, $rCo^{2+} = 0.0745$ nm), leading to a decrease in crystallite size. The average crystal sizes on the thin films are found to vary from 40 to 50 nm, and the Al dopant concentration decreases the crystallite size of the thin films.

Fig. 5 (a & b) show micrographs of the surfaces and thicknesses of ZnO and Co,Al:ZnO films. A uniform grain size distribution is also seen on the thin films
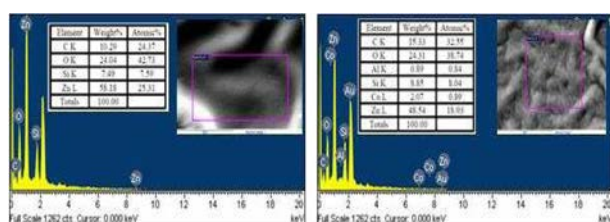
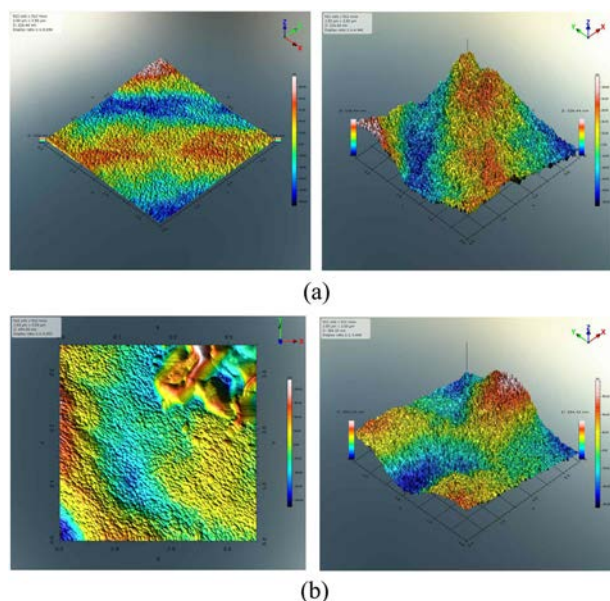**Fig. 6.** EDS spectra of ZnO and Co,Al:ZnO thin films.

Fig. 7. AFM micrographs of (a) ZnO and (b) Co,Al:ZnO thin film surfaces.

deposited over glass substrates by spin coating. However, the films show a minute porous contrast, which indicates that the pores in the surface are related with the decomposition reaction of the precursor and the evaporation of residual organics in thin films. The grains in the Co, Al:ZnO films are smoother than in pure ZnO. According to the cross-sectional observations, the thickness of the films is in the order of 650-700 nm. The average grain size of the particulates of about 50 nm is obtained and it is in good agreement with the particle size calculated from XRD peak broadening method. The EDS spectra in fig. 6 show the existence of Co, Al, Zn and O apart from C and Si peaks which are due to the conductive carbon surface during sample preparation and glass substrate, respectively. From these spectra, it is found that the Co,Al:ZnO ratio is close to the stoichiometric and in good agreement with the nominal chemical composition.

Fig. 7 presents the AFM images of pure and Co, Al co-doped zinc oxide thin films annealed at 500 ℃. The micrographs exhibit a homogeneous distribution of grains with a lack of grain boundaries. The annealed thin films consist of regions with a very fine, spherical and uniform grain structure. The size of the grains varied from 40-60 nm for pure ZnO and 30-50 nm for Co, Al:ZnO thin films. The doping treatment reveals a
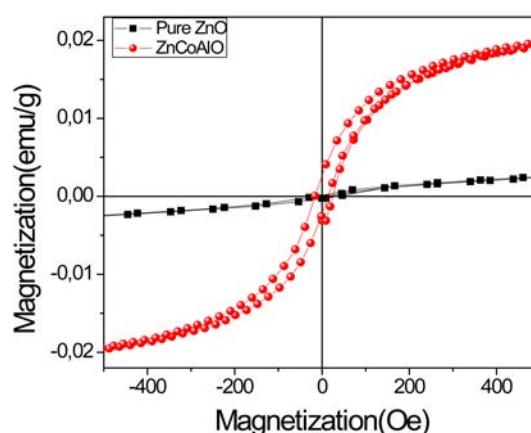

Fig. 8. Field dependent magnetization of pure and Co,Al:ZnO thin films.

finer topography and crack free thin films.

For the sol-gel spin coated Co,Al:ZnO thin film, magnetic hysteresis studies were carried out at room temperature (300 K) using VSM. The diamagnetic nature of the sample holder was calibrated without the samples, because the dilute magnetic semiconductors exhibit weaker magnetization. All the measurements exhibit a zoom in the apparent hysteresis which actually appears. Fig. 8 shows room temperature magnetic hysteresis curves for pure ZnO and Co, Al co-doped ZnO thin films. But it is difficult to give an approximate value of coercivity since it is in the order of 10-20 Oe. The field dependent magnetization curves for the pure ZnO shows a very low paramagnetic behavior which is negligible and it is regarded as diamagnetic. This data show a clear ferromagnetic behavior for the sample which is doped with Co. However, the pure ZnO shows a super diamagnetic behavior without any hysteresis at room temperature. The ferromagnetism in the Co, Al co-doped ZnO thin films could `be due to the exchange coupling between localized `d` spins on the Co ions mediated by free delocalized carriers [15], and it is expected to be considered as a promising material for spintronics.

Conclusions

Pure and Co, Al co-doped zinc oxide thin films were fabricated by a sol-gel spin coating technique and crack free films were obtained after annealing at 500 ℃. The thermal analysis of the precursor solution revealed the decomposition of organic volatiles and formation of the metal oxide during the heat treatment. In structural studies, same lattice planes were observed for both pure and Co, Al doped ZnO, and also polycrystalline single-phase ZnO with the hexagonal wurtzite structure and it confirms the substitution of Co and Al into ZnO. The average grain sizes on the thin films were found to vary slightly from 40-50 nm and the thickness of the films was in the range of 650-700 nm. The SEM and

AFM micrographs show the films possess a uniform homogenous distribution of grains. The EDS spectra confirmed the formation of Co,Al:ZnO films and the detected elemental ratio was close to the stoichiometric proportion. The field dependent magnetization of pure ZnO and Co, Al co-doped ZnO exhibited diamagnetic and ferromagnetic behavior, respectively at room temperature.

Acknowledgement

References

1. K.Y. Kong, Y. Ding, R. Yang, Z.L. Wang, Science 303 (2004) 1348.
2. T. Shiosaki, N. Kitamura, A. Kawabata, in: Proceedings of the IEEE Ultrasonic Symposium 296 ff (1991).
3. K. Zhang, F. Zhu, C.H.A. Huan, A.T.S. Wee, T. Osipowicz, Surf. Interf. Anal. 28 (1999) 271.
4. T. Dietl, H. Ohno, F. Matsukura, J. Cubert, D. Ferrand, Science 287 (2000) 1019.
5. H. Ohno, Science 281 (1998) 951.
6. S.A. Wolf, D.D. Awschalom, R.A. Buhrman, J.M. Daughton, S. von Molnar, M.L. Roukes, A.Y. Chtchelkanova, D. Treger, Science 294 (2001) 1488.
7. M. Venkatesan, P. Stamenov, L.S. Dorneles, R.D. Gunning, B. Bernoux, J.M.D. Coey, Appl. Phys. Lett. 90 (2007) 242508.
8. A.J. Behan, A. Mokhtari, H.J. Blythe, D. Score, X.H. Xu, J.R. Neal, A.M. Fox, D.A. Gehring, Phys. Rev. Lett. 100 (2008) 047206.
9. T. Minami, Thin Solid Films 516 (2008) 5822.
10. B.S. Chua, S. Xu, Y.P. Ren, Q.J. Cheng, K. Ostrikov, J. Alloys Compd. 485 (2009) 379.
11. W. Gao, Z.W. Li, J. Alloys Compd. 449 (2008) 202.
12. M.H. Huang, S. Mao, H. Feick, H. Yan, Y. Wu, H. Kind, E. Weber, R. Russo, P. Yang, Science 292 (2001) 1897.
13. P. Scherrer, Göttinger Nachrichten Gesell. 2 (1918) 98.
14. S. Fujihara, A. Suzuki, T. Kimura, J. Appl. Phys. 94 (2003) 2411.
15. B. Pandey, S. Ghosh, P. Srivastava, D.K. Avasthi, D. Kabiraj, J.C. Pivin, J. Mag. Mag. Mater. 320 (2008) 3347.